

Phosphatidylinositol 3-Kinase Hyperactivation Results in Lapatinib Resistance that Is Reversed by the mTOR/Phosphatidylinositol 3-Kinase Inhibitor NVP-BEZ235

Pieter J.A. Eichhorn,¹ Magüi Gili,¹ Maurizio Scaltriti,¹ Violeta Serra,¹ Marta Guzman,¹ Wouter Nijkamp,² Roderick L. Beijersbergen,² Vanesa Valero,¹ Joan Seoane,^{1,3,4} René Bernards,² and José Baselga^{1,3}

¹Medical Oncology Program, Vall d'Hebron Institut de Oncologia, Barcelona, Spain; ²Division of Molecular Carcinogenesis and Center for Biomedical Genetics, The Netherlands Cancer Institute, Amsterdam, the Netherlands; ³Autonomous University of Barcelona, Barcelona; and ⁴Institució Catalana de Recerca i Estudis Avançats (ICREA), Barcelona, Spain

Abstract

Small molecule inhibitors of HER2 are clinically active in women with advanced HER2-positive breast cancer who have progressed on trastuzumab treatment. However, the effectiveness of this class of agents is limited by either primary resistance or acquired resistance. Using an unbiased genetic approach, we performed a genome wide loss-of-function short hairpin RNA screen to identify novel modulators of resistance to lapatinib, a recently approved anti-HER2 tyrosine kinase inhibitor. Here, we have identified the tumor suppressor PTEN as a modulator of lapatinib sensitivity *in vitro* and *in vivo*. In addition, we show that two dominant activating mutations in PIK3CA (E545K and H1047R), which are prevalent in breast cancer, also confer resistance to lapatinib. Furthermore, we show that phosphatidylinositol 3-kinase (PI3K)-induced lapatinib resistance can be abrogated through the use of NVP-BEZ235, a dual inhibitor of PI3K/mTOR. Our data show that deregulation of the PI3K pathway, either through loss-of-function mutations in PTEN or dominant activating mutations in PIK3CA, leads to lapatinib resistance, which can be effectively reversed by NVP-BEZ235. [Cancer Res 2008;68(22):9221–30]

Introduction

The HER2 (ErbB2/neu) gene is amplified/overexpressed in 20% to 30% of invasive breast carcinomas with its overexpression being associated with increased metastatic potential and poor clinical outcome (1, 2). As a result HER2 is an attractive target for therapeutic drug development. A myriad of inhibitors targeting HER2 have been developed, most notably, the humanized monoclonal antibody trastuzumab (Herceptin), which targets the extracellular domain of HER2. The mechanisms underlying trastuzumab activity include down-regulation of HER2 expression via endocytosis (3), deregulation of the phosphatidylinositol 3-kinase (PI3K)-AKT pathway, either through disruption of HER2 signaling or by increased PTEN membrane localization (4), or the induction of a G₁ growth arrest through the stabilization of the cyclin-dependent kinase inhibitor p27 (5). Interestingly, trastuzu-

ma has also been shown to induce apoptosis in multiple breast cancer cell lines via antibody-dependent cell-mediated cytotoxicity (6). Clinical studies have established that trastuzumab provides substantial clinical benefits in patients with HER2-overexpressing metastatic breast cancers. However, the objective response rate to single-agent trastuzumab is low, with only 12% to 34% of patients responding to monotherapy (7, 8).

A number of mechanisms have been identified, which consequently limit the effect of trastuzumab-based therapy in patients, including hyperactivation of HER2 family members or the dimerization of HER2 with the insulin-like growth factor-I (IGF-I) receptor (IGFRI; refs. 9, 10). Furthermore, the recent identification of a truncated form of the HER2 receptor that lacks the extracellular trastuzumab-binding domain (p95 CTF) has been reported to affect trastuzumab sensitivity (11).

Mutations in PIK3CA have been reported to occur at high frequency in a number of human cancers (12). Increasing evidence indicates that a functional PI3K-AKT pathway is also critical for trastuzumab sensitivity. Hyperactivation of PI3K signaling, downstream from HER2, either through loss-of-function PTEN mutations or dominant activating mutations in the catalytic subunit of PI3K, PIK3CA α , seems to decrease trastuzumab activity in breast cancer (4, 13). Interestingly, in primary breast cancer, a significant correlation between HER2 overexpression and the presence of PI3K mutations has been described, insinuating that multiple oncogenic inputs are required to overcome the strong tumor suppressor capability of wild-type (wt) PTEN (14).

Lapatinib is an orally active small molecule inhibitor of the epidermal growth factor receptor (EGFR) and HER2 tyrosine kinase domains. Treatment with lapatinib has been shown to deregulate baseline and ligand-stimulated HER2 activity, resulting in the inhibition of downstream effector pathways (15). Initial experiments have shown that lapatinib potently inhibits cell survival in trastuzumab-resistant breast cancer cells through the induction of apoptosis (16, 17). Furthermore, in contrast to trastuzumab, lapatinib effectively inhibits the transactivation of EGFR and HER2 by IGF-I signaling (16). Recent data has also described the ability of lapatinib to potently inhibit the tumor forming potential of p95 CTF-derived breast cancer cell lines in mouse xenograft models (11).

A series of clinical trials has shown that lapatinib is active in patients with HER2 overexpressing breast cancer, and a pivotal phase III study in patients with advanced disease has shown that lapatinib, in combination with capecitabine, prolongs progression-free survival in patients who have progressed on trastuzumab (18, 19). However, as with trastuzumab, patients with advanced disease who initially respond to this TKI almost

Note: Supplementary data for this article are available at Cancer Research Online (<http://cancerres.aacrjournals.org/>).

Requests for reprints: José Baselga, Vall d'Hebron University Hospital, P. Vall d'Hebron 119, Barcelona, 08035 Spain. Phone: 01134-932746085; Fax: 01134-932746059; E-mail: jbaselga@vhebron.net.

©2008 American Association for Cancer Research.
doi:10.1158/0008-5472.CAN-08-1740

invariably develop resistance. Therefore, a clear understanding of the mechanisms underlying lapatinib secondary or acquired resistance will be advantageous on deciding which patients may benefit the most. Moreover, prior identification of patients who are unlikely to respond to lapatinib therapy due to upfront or primary resistance may lead to the development of rational drug combinations that are likely to circumvent resistance. Here, using an unbiased functional genetic approach, we have identified that dominant activating mutations in the PI3K pathway lead to lapatinib resistance *in vitro* and *in vivo*. Furthermore, we show that the combination therapy of lapatinib plus the dual PI3K/mTOR inhibitor NVP-BEZ235 leads to the complete growth arrest in PI3K pathway-induced lapatinib resistance.

Materials and Methods

Short hairpin RNA barcode screen. The pooled NKI library representing 23,742 vectors was retrovirally infected into BT474 cells and selected with puromycin (2.0 $\mu\text{g}/\text{mL}$) for 3 d. After selection, cells were trypsinized and plated into two populations at a density of 2×10^5 in a 15-cm dish. A total of 2×10^6 cells were plated for each population. One population remained untreated, whereas the other population was cultured in 27 nmol/L lapatinib. Medium was refreshed every 3 d. After 2 wk, cells were trypsinized and replated out at 2×10^5 in a 15-cm dish. After a total of 4 wk in culture, the treated and untreated populations were collected and genomic DNA was isolated using DNAzol (Life Technologies). The short hairpin RNA (shRNA) inserts were amplified from genomic DNA by PCR. Primers used for PCR are as follows: forward, GGC CAG TGA ATT GTA ATA CGA CTC ACT ATA GGG AGG CGG CCC TTG AAC CTC CTC GTT CGA CC; reverse, TAA AGC GCA TGC TCC AGA CT. Purified PCR products were used for linear RNA amplification, and purified products were labeled with cyanine-3 or cyanine-5 fluorescent isotopes (Kreatech). Labeled RNA probes from both untreated and lapatinib-treated cells were combined and hybridized to microarrays. Quantification of the microarray images was performed with Image 5.6 (Biodiscovery). Microarray data were normalized and \log_2 transformed. Barcode protocols can be accessed online.³

Plasmids and antibodies. pJP1520, pJP1520-PIK3CA α , pJP1520-E545K, and pJP1520-H1047R were kind gifts from Joan Brugge. The second PTEN hairpin was a kind gift from Roderik Kortlever. The antibodies anti-phosphorylated AKT (S⁴⁷³), anti-phosphorylated AKT (S³⁰⁸), anti-phosphorylated extracellular signal-regulated kinase (ERK), anti-phosphorylated S6^{240/244}, anti-S6, IRS1, and PTEN were from Cell Signaling. Anti-AKT and anti-ERK were purchased from Santa Cruz. Anti-tubulin was purchased from Sigma Aldrich. Anti-pTyr was purchased from Upstate.

Cell culture and transient transfections. The HER2-positive cell lines BT474 [PTEN+, PI3K(K111N), KRAS wt, HRAS wt, NRAS wt] and SkBR3 (PTEN +, PI3K wt, p53 mutant, KRAS wt, HRAS wt, NRAS wt) cells were cultured in DMEM-F12 + Glutamax, whereas phoenix cells were cultured in DMEM. Both media were supplemented with 10% FCS and penicillin/streptomycin. Phoenix cells were divided in 10-cm dishes 1 d before transfection. Subconfluent cells were transfected with 25 μg of pRetroSuper DNA using the calcium phosphate transfection method (20). Cells were incubated overnight and washed twice in PBS. At 48 h after transfection, the viral supernatant was collected, purified with a 45- μm filter, and supplemented with polybrene (0.8 $\mu\text{g}/\text{mL}$). Infection of desired cells was repeated three to five times. Infected cells were selected with puromycin (2 $\mu\text{g}/\text{mL}$) for 3 d. When desired, stable cell lines were treated with trastuzumab (5 $\mu\text{g}/\text{mL}$; Herceptin, kindly provided by Genentech, Inc.), lapatinib (27 nmol/L; Tykerb, kindly provided by GlaxoSmithKline), or NVP-BEZ235 (15 nmol/L; kindly provided by Novartis), or in combination overnight unless otherwise indicated. PI-103 was purchased from Echelon Biosciences.

Commasie staining. BT474 or SkBR3 cells were cultured in the presence of trastuzumab (5 mg/mL), lapatinib (27 nmol/L), or both for 3 to 4 wk. Cells were washed twice in PBS and fixed with methanol and acetic acid (3:1). After 30 min, cells were washed once in water, and 10 mL commassie stain (0.2% commassie, 50% methanol, and 10% acetic acid) were added. After 30 min, cells were washed thrice in H₂O and air-dried.

Western blotting. Cells were lysed in solubilizing buffer [50 mmol/L Tris (pH 8.0), 150 mmol/L NaCl, 1% NP40, 0.5% deoxycholic acid, 0.1% SDS, 1 mmol/L sodium vanadate, 1 mmol/L PPI, 50 mmol/L sodium fluoride, 100 mmol/L β -glycerol phosphate], supplemented with protease inhibitors (Complete, Roche). Whole-cell extracts were then separated on 7% to 12% SDS-PAGE gels and transferred to polyvinylidene difluoride membranes (Millipore). Membranes were blocked with bovine serum albumin (BSA) and probed with specific antibodies. Blots were then incubated with a horseradish peroxidase-linked second antibody and resolved with chemiluminescence (Pierce).

Growth curves. BT474 cells were retrovirally infected and selected, and polyclonal cell lines were seeded in 12-well plates (2×10^4). At 24 h later, cells were treated with either 27 nmol/L lapatinib, 5 $\mu\text{g}/\text{mL}$ trastuzumab, or 15 nmol/L NVP-BEZ235 where appropriate. Cell numbers were quantified at the indicated time points by fixing cells with 4% glutaraldehyde, washing the cells twice in H₂O, and staining the cells with crystal violet (0.1% Sigma). The dye was subsequently extracted with 10% acetic acid, and its absorbance was determined (570 nm). Growth curves were performed in triplicate.

Tumor xenografts in nude mice. Mice were maintained under the institutional guidelines set by the Vall d'Hebron University Hospital Care and Use Committee. Six- to eight-week-old female BALB/c athymic mice (nu⁻/nu⁺, $n = 32$) were acquired from Charles Rivers Laboratories. Mice were housed in air-filtered laminar flow cabinets with a 12-h light cycle and food and water ad libitum. Mice were acclimatized for 2 wk. A 17 β -estradiol pellet (Innovative Research of America) was inserted s.c. to each mouse 1 d before injection with BT474 VH2 (pRS-GFP) or BT474 VH2 (pRS-PTEN-B; ref. 21). For BT474 VH2 clones, 2×10^7 cells were injected s.c., and treatment was initiated when the tumors achieved a mean size of 400 mm³. Lapatinib was given daily by oral gavage in 0.5% hydroxypropylmethylcellulose, 0.1% Tween 80. Tumor xenografts were measured with calipers every 2 to 3 d, and tumor volume was determined using the formula: (length \times width²) \times ($\pi / 6$). When appropriate, mice were anesthetized with 1.5% isoflurane-air mixture and killed by cervical dislocation. Tumors were homogenized in solubilizing buffer (see above).

Results

Loss of PTEN expression confers resistance to Lapatinib. To identify genes whose suppression by shRNA cause resistance to lapatinib, we infected BT474 HER2 overexpressing breast cancer cells with a retroviral library that comprises 23,742 shRNA vectors targeting 7,914 genes (22). After selection with puromycin, cells were plated out at low density and treated with 27 nmol/L lapatinib. The IC₅₀ value of BT474 cells was predetermined to be ~ 25 nmol/L (data not shown; refs. 17, 23). To rapidly identify shRNAs that are capable of circumventing the proliferation arrest induced by lapatinib, we used shRNA barcode technology (24). After 4 weeks, DNA was harvested from the surviving lapatinib-treated cells and, as control, from untreated cells (Supplementary Fig. S1A). shRNA cassettes were recovered by PCR, and RNA probes were generated by linear amplification and fluorescent labeling. The relative representation of each shRNA in the population was measured using a microarray. To minimize experimental variation, we combined the data from two individual experiments. Supplementary Fig. S1B shows the relative abundance of the shRNA vectors in the lapatinib-treated population compared with untreated controls. Interestingly, we identified eight shRNA vectors (C200RF44, DNMT3A, GRAP2, PPP1R14B, PTEN, TK1, ZAP70, and

³ <http://screeninc.nki.nl/>

ZIC3) for which the same shRNA vector was identified in both individual barcode screens (Supplementary Tables S1 and S2). However, when tested in second round selection of the eight shRNA vectors tested, only the hairpin targeting PTEN conferred resistance to lapatinib (Fig. 1A; data not shown). As expected, loss of PTEN expression also abrogated trastuzumab sensitivity (Fig. 1A). Critically, a second nonoverlapping shRNA, capable of inhibiting PTEN expression (Fig. 1B), also conferred resistance to lapatinib and trastuzumab, therefore arguing against an off-target effect (Fig. 1A; ref. 25). An shRNA targeting GFP was used as a negative control in all experiments. Interestingly, treatment with both trastuzumab and lapatinib conferred an enhanced response to the proliferation potential of HER2-positive cells compared with either treatment alone, confirming the results of others, which have indicated that combining lapatinib with trastuzumab enhances their biological effect (Fig. 1A; ref. 26). However, whereas combination treatment with lapatinib and trastuzumab limited cellular proliferation in PTEN knockdown cells, viable cells remained (Fig. 1A).

To investigate the sensitivity of the PTEN knockdown cell lines to the different HER2-targeted therapies, we analyzed the proliferation potential of PTEN knockdown cells when treated with trastuzumab (5 µg/mL), lapatinib (27 nmol/L), or both for 4 weeks. Treatment with HER2-directed therapies completely

inhibited the proliferation potential of control cells. However, the ablation of PTEN expression in BT474 cells decreased the growth inhibitory properties of both trastuzumab and lapatinib (Fig. 1C). Collectively these data suggest that PTEN expression is required for both trastuzumab and lapatinib sensitivity in BT474 cells.

As has previously been reported, lapatinib growth inhibition correlates with the down-regulation of HER2-dependent PI3K signaling (17, 26). Therefore, to study the effects of lapatinib on PI3K signaling in cells that lack PTEN activity, we treated BT474 cells or BT474 PTEN-depleted cells with lapatinib (Fig. 1D). Indeed, similar to trastuzumab, there was a significant down-regulation in AKT⁴⁷³ phosphorylation in lapatinib-treated control cells compared with untreated control cells. In contrast down-regulation of AKT phosphorylation was attenuated in lapatinib-treated PTEN knockdown cells compared with lapatinib-treated controls. However, unlike trastuzumab, no change was observed in mitogen-activated protein kinase (MAPK) phosphorylation upon treatment with lapatinib. In addition, treatment of cells with both lapatinib and trastuzumab resulted in an additive inhibitory effect on AKT activity, suggesting that trastuzumab and lapatinib may function through partially nonoverlapping mechanisms to disrupt HER2-dependent PI3K signaling.

The approved dose in patients of lapatinib, when used in combination with capecitabine, is a daily dose of 1,250 mg (18).

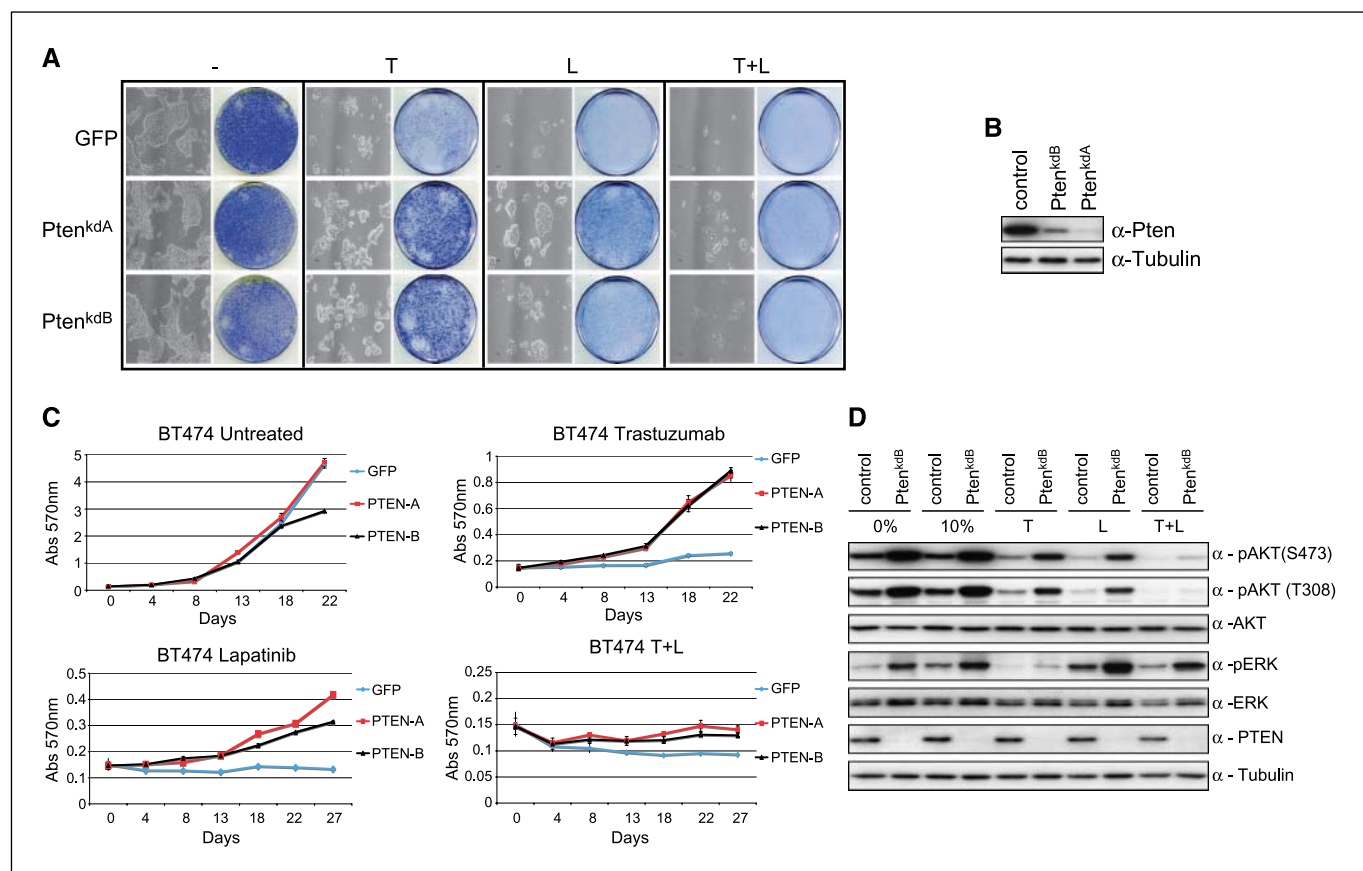


Figure 1. PTEN silencing decreases sensitivity to trastuzumab and lapatinib. When required cells were either treated with trastuzumab (5 µg/mL) or lapatinib (27 nmol/L), unless otherwise stated. **A**, colony formation assay in BT474 cells infected with either NK1 library vector PTEN^{k_dA}, a second independent shRNA vector PTEN^{k_dB}, or relevant controls. Infected cells were left untreated or treated with trastuzumab, or lapatinib, or both. After 4 wk, cells were photographed and stained with crystal violet. **B**, Western blot analysis monitoring PTEN expression in stably infected PTEN knockdown cells. **C**, growth curves of stably infected PTEN knockdown BT474 cells treated for 3 wk with trastuzumab, lapatinib, or both. Cell numbers were quantified as described in Materials and Methods. Growth curves were performed in triplicate. *Points*, mean; *bars*, SD. **D**, Western blot analysis of stably infected BT474 cells with shRNA PTEN^{k_dB} vector treated overnight with trastuzumab, lapatinib, or both in 10% serum. Whole-cell extracts were analyzed with the indicated antibodies.

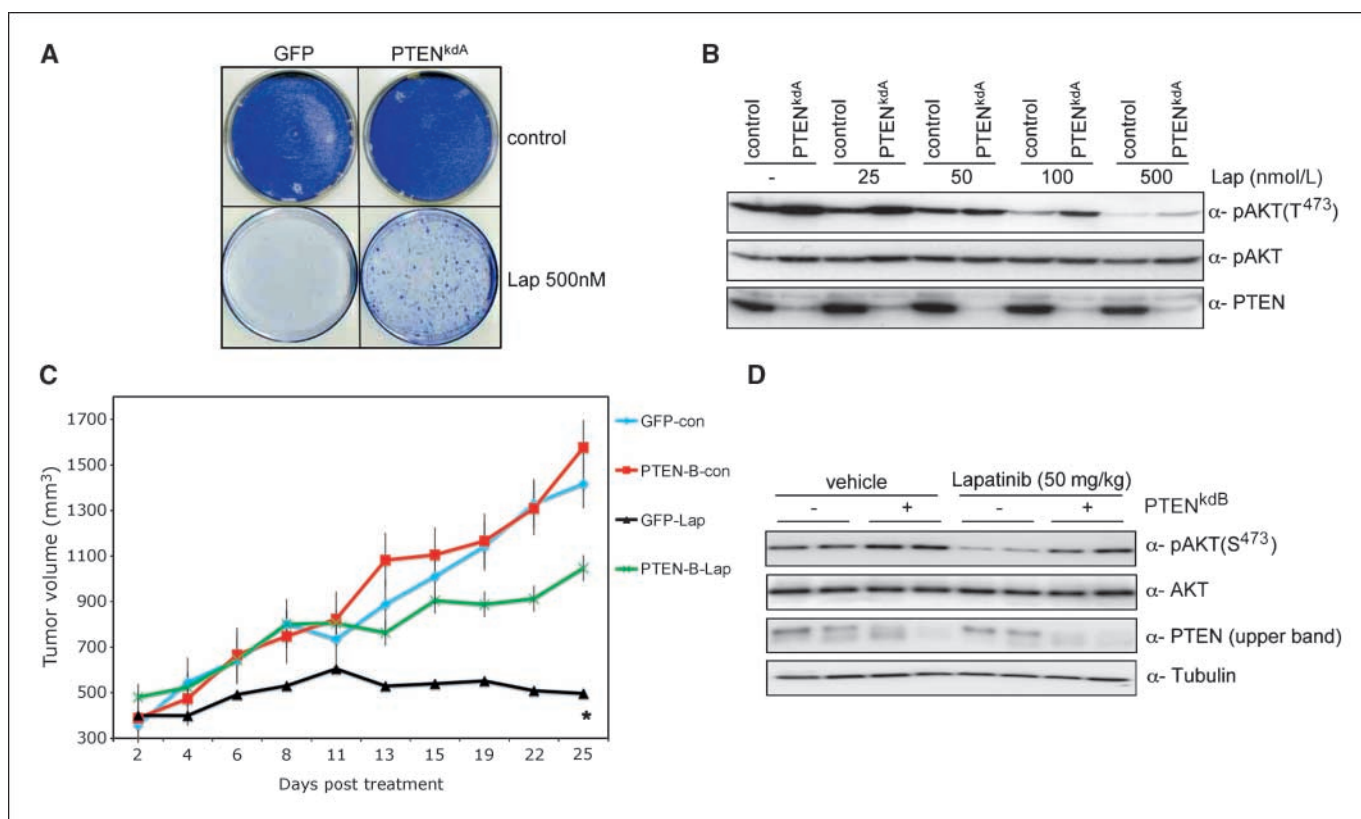


Figure 2. PTEN silencing decreases sensitivity to lapatinib at clinically relevant concentrations. **A**, colony formation assay in BT474 cells infected with vector PTEN^{k_dA}. Infected cells were left untreated or treated with lapatinib (500 nmol/L). After 4 wk (controls) or after 12 wk (lapatinib treated), cells were photographed and stained with crystal violet. **B**, phosphorylated AKT (pAKT) in relation to the total level of unphosphorylated protein in lapatinib-treated samples (0, 25, 50, 100, 500 nmol/L) in the presence or absence of PTEN^{k_dA} vector. **C**, mouse xenograft assay with BT474 VH2 cells stably infected with vector PTEN^{k_dB} or relevant controls. Mice were treated daily with lapatinib (50 mg/kg) or vehicle. Points, mean tumor volume; bars, SE. A two-tailed Student's *t* test compares the two treated populations. *, *P* < 0.02. **D**, Western blot analysis of mouse xenograft BT474 VH2 tumors stably infected with vector PTEN^{k_dB} or relevant controls. Whole-cell extracts were analyzed with indicated antibodies.

This dosage results in a minimal plasma drug concentration of ~500 nmol/L (27). Therefore, to test if PTEN loss can overcome lapatinib sensitivity at clinically relevant concentrations, we performed a colony formation assay. As shown in Fig. 2A, loss of PTEN expression significantly enhanced the growth potential of BT474 cells when treated at clinically relevant doses of lapatinib, which correlates with an increase in AKT activity (Fig. 2B).

To investigate if PTEN deficiency leads to lapatinib resistance *in vivo*, we retrovirally infected BT474 cells with an shRNA-targeting PTEN or a relevant control and injected athymic nude mice s.c. When tumor xenografts reached a mean size of 400 mm³ (~14 days), we treated the mice with lapatinib (50 mg/kg) or vehicle daily. BT474 PTEN-depleted cells exhibited similar growth rates to controls in vehicle-treated mice (Fig. 2C). However, loss of PTEN significantly inhibited the antitumorigenic effects of lapatinib compared with controls (Fig. 2C). Furthermore, Western blot analysis of tumors clearly shows a decrease in AKT dephosphorylation in PTEN knockdown tumors compared with controls (Fig. 2D). Together, these data show that loss of PTEN expression attenuates lapatinib sensitivity *in vitro* and *in vivo* possibly by maintaining the activation of the AKT signaling pathway.

Breast cancer–relevant PI3K mutations confer resistance to lapatinib. The PI3K pathway is frequently mutated in cancer. Loss-of-function mutations in PTEN have been described in a variety of cancers, resulting in hyperactivation of the PI3K pathway

(28). In addition, a number of recent reports have indicated that activating mutations in PI3K subunit PIK3CA occur in 18% to 40% of primary breast cancers (29). The majority of these mutations reside within two hotspot regions, leading to single amino acid substitutions within the helical domain (E545K) and kinase domain (H1047R) resulting in enhanced PI3K signaling (30). Importantly, deregulation of the PI3K pathway seems to be a poor prognostic indicator toward trastuzumab sensitivity (13).

To investigate whether cancer-associated PI3K mutations result in lapatinib resistance, we retrovirally transduced BT474 cells with hemagglutinin (HA)-tagged PIK3CA or the breast cancer-relevant isoforms, HA-E545K, or HA-H1047R. Both PI3K-dominant activating mutations rendered BT474 cells nearly completely refractory to the growth inhibitory effects of lapatinib and trastuzumab (Fig. 3A). However, unlike trastuzumab, lapatinib seems to limit the growth potential of PIK3CA-overexpressing BT474 cells (Fig. 3A). Interestingly, expression of PIK3CA (E545K) and PIK3CA (H1047R) also conferred resistance to the growth arrest conferred by the combined treatment of lapatinib and trastuzumab (Fig. 3A). Similar results were observed in the HER2-overexpressing cell line SKBR3 (Supplementary Fig. S2).

Next, we analyzed the proliferation potential of BT474 cells retrovirally infected with the different PI3K alleles when treated with trastuzumab (5 μg/mL), lapatinib (27 nmol/L), or both for 3 weeks. As expected, expression of activated PI3K mutants abrogated the growth inhibitory effects of these anti-HER2

therapies when used as treatment, either alone or in combination (Fig. 3B). In contrast, in PIK3CA α -overexpressing cells, both trastuzumab and lapatinib were active although lapatinib was superior at the concentrations tested (Fig. 3B). In cells harboring mutant PI3K, there was no difference in proliferation relative to wt expressing cells in nontreated samples. Together, these data suggest that PI3K breast cancer prevalent mutations can counteract lapatinib and trastuzumab sensitivity in HER2-positive cells.

Because both PTEN loss-of-function mutations and oncogenic mutations in PI3K leads to constitutive AKT signaling, we reasoned that AKT inhibition by lapatinib might be attenuated in the presence of dominant activating mutations in PI3K (29, 31). Indeed, both E545K and H1047R mutant alleles bypassed the inhibitory effects of lapatinib and trastuzumab on AKT activity as measured by AKT^{S473} phosphorylation (Fig. 3C). Consistent with this, both E545K and H1047R mutants decreased the sensitivity of lapatinib toward AKT activity at clinically relevant concentrations (Fig. 4C and D), resulting in a marked increase in cellular survival (Fig. 4A). In contrast, no difference was observed in

phosphorylated AKT levels in PIK3CA α -overexpressing cells compared with controls in lapatinib-treated samples (Fig. 3C). Collectively, these data suggest that hyperactivation of the PI3K-AKT pathway by hotspot mutations is a critical regulator of the anti-HER2 therapies, trastuzumab and lapatinib. Interestingly, whereas similar effects were observed in PIK3CA α overexpressing cells treated with trastuzumab, only a minor degree of resistance was noted in lapatinib-treated samples.

Lapatinib and the PI3K inhibitor NVP-BE2235 collaborate to suppress the PI3K-AKT-mTOR axis driven by loss-of-function PTEN mutations. The above data clearly shows that hyperactivation of the PI3K pathway confers lapatinib resistance. Therefore, we reasoned that the use of PI3K antagonists would restore the sensitivity of HER2-directed therapies. To do this, we made use of the dual PI3K/mTOR inhibitor NVP-BE2235. NVP-BE2235 is an imidazo[4,5-c]quinoline derivative that binds equivalently to the ATP-binding cleft of these enzymes and is presently undergoing phase I clinical trials (32). Of note, we have recently reported that the IC₅₀ for phosphorylated Akt (Ser⁴⁷³) was 6.4-fold higher than that of phosphorylated S6

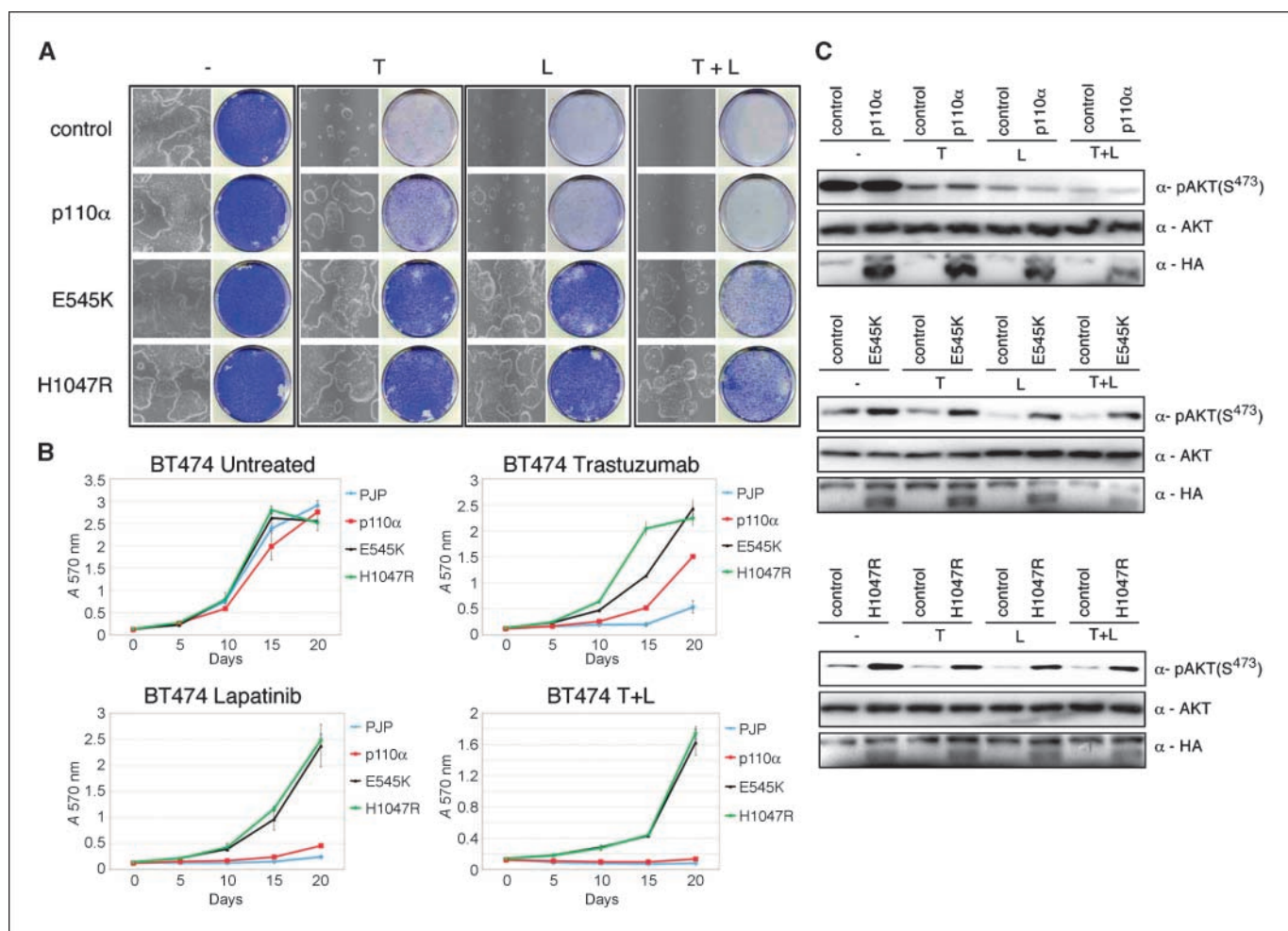


Figure 3. Constitutive activation of the PI3K pathway decreases sensitivity to trastuzumab and lapatinib. When required, cells were treated with either trastuzumab (5 μ g/mL) or lapatinib (27 nmol/L), unless otherwise stated. *A*, colony formation assay in BT474 cells infected with either wt PIK3CA α or PIK3CA α mutants E545K and H1047R or relevant controls. Infected cells were treated with trastuzumab, lapatinib, or both. After 4 wk, cells were photographed and stained with crystal violet. *B*, growth curves of stably infected PI3K wt or mutant PIK3CA α BT474 cells treated for 3 wk with trastuzumab, lapatinib, or both. Cell numbers were quantified as described in Materials and Methods. Growth curves were performed in triplicate. Points, mean; bars, SD. *C*, Western blot analysis of BT474 cells infected with HA-tagged PI3K PIK3CA α (top left), PI3K(E545K) PIK3CA α (lower left), PI3K(H1047R) PIK3CA α (right), or controls were treated overnight with trastuzumab, lapatinib, or both. Whole-cell extracts were analyzed with indicated antibodies.

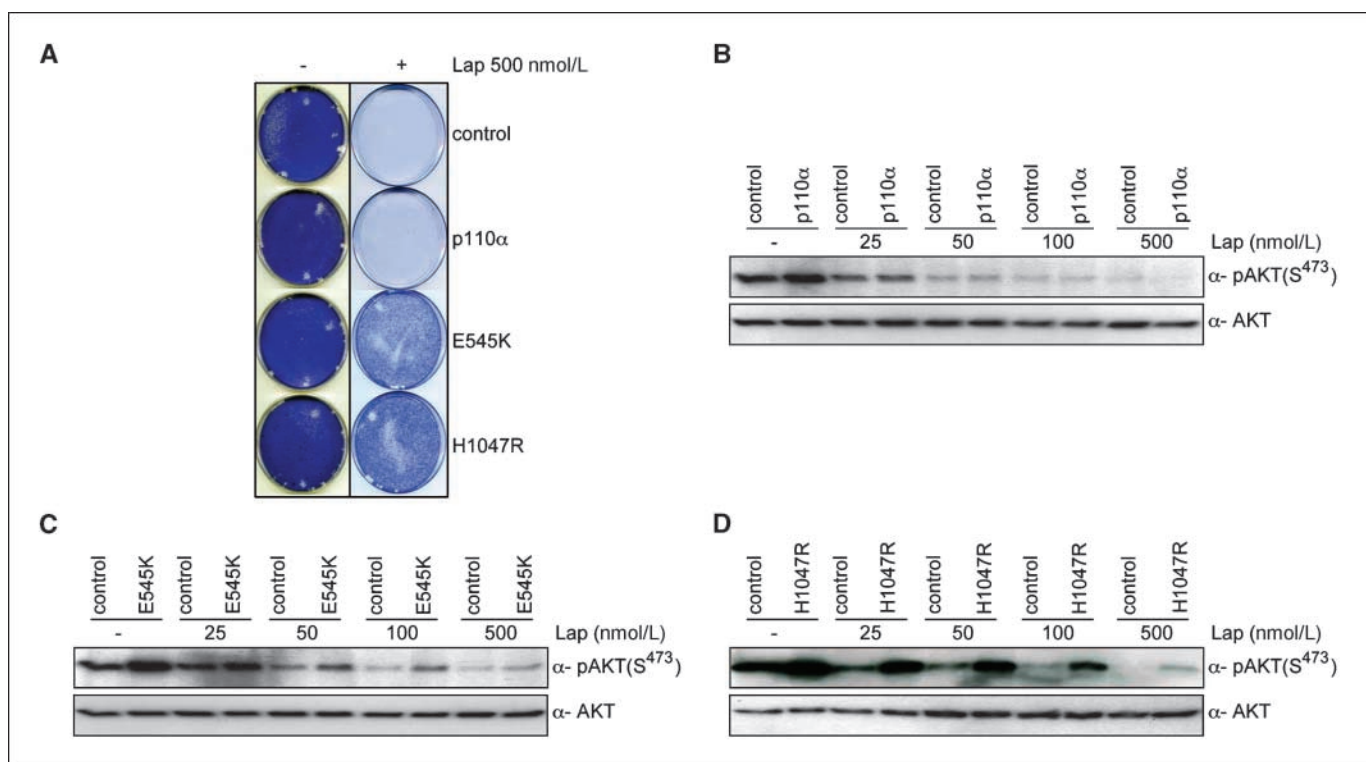


Figure 4. Constitutive activation of the PI3K pathway decreases sensitivity to lapatinib at clinically relevant concentrations. **A**, colony formation assay in BT474 cells infected with either wt PIK3CA α or PIK3CA α mutants E545K and H1047R or relevant controls. Infected cells were left untreated or treated with lapatinib (500 nmol/L). After 5 wk, cells were photographed and stained with crystal violet. **B**, Western blot analysis showing phosphorylated AKT (*pAKT*) in relation to the total level of unphosphorylated protein in lapatinib-treated samples (0, 25, 50, 100, 500 nmol/L) in the presence or absence of wt PIK3CA α vector. **C**, Western blot analysis showing phosphorylated AKT in relation to the total level of unphosphorylated protein in lapatinib-treated samples (0, 25, 50, 100, 500 nmol/L) in the presence or absence of PIK3CA α mutant E545K. **D**, Western blot analysis showing phosphorylated AKT in relation to the total level of unphosphorylated protein in lapatinib-treated samples (0, 25, 50, 100, 500 nmol/L) in the presence or absence of PIK3CA α mutant H1047R.

(77 ± 29 nmol/L compared with 12 ± 10 nmol/L) in NVP-BE2235-treated samples (33).

Stably infected BT474 PTEN knockdown cells were treated with either trastuzumab (5 mg/mL), lapatinib (27 nmol/L), NVP-BE2235 (15 nmol/L), or in combination. The IC_{50} value for NVP-BE2235 in BT474 cells is ~ 15 nmol/L (data not shown). As shown in Fig. 5A, BT474 cells are exquisitely sensitive to NVP-BE2235 treatment alone, which is only slightly improved by the addition of trastuzumab or lapatinib. In contrast and in line with previous observations, BT474 PTEN knockdown cells inhibited trastuzumab, lapatinib, or NVP-BE2235-mediated growth inhibition compared with control cells. However, combination treatment in BT474 PTEN knockdown cells with either trastuzumab and NVP-BE2235 or lapatinib and NVP-BE2235 was additive (Fig. 5A). Similar observations were noted when we analyzed the proliferation potential of BT474 cells expressing hairpins targeting PTEN exposed to either lapatinib, NVP-BE2235, or the combination (Fig. 5B).

To elucidate the mechanisms behind the additive effect observed between lapatinib and NVP-BE2235, we compared the intercellular responses of BT474 or BT474 PTEN-depleted cells treated with lapatinib or NVP-BE2235 alone or in combination (Fig. 5C). In wt cells, as expected, HER2 inhibition by lapatinib reduced phosphorylation of AKT⁴⁷³ and downstream mTOR signaling exhibited by reduced S6^{240/244} phosphorylation. Similarly, NVP-BE2235 (100 nmol/L) treatment reduced phosphorylation of both AKT⁴⁷³ and S6^{240/244}, which was accompanied by an increase in the

phosphorylation of ERK in control cells, but not in PTEN knockdown cells (Fig. 5C). Similar observations were seen with another dual PI3K/mTOR inhibitor, PI-103, albeit at higher concentrations (Supplementary Fig. S3A and B). Recent data show that mTOR inhibition results in a mobility shift of IRS1 due to decreased serine phosphorylation (34). The loss of IRS1 serine phosphorylation inhibits degradation of the protein. Consequently, IRS1 is phosphorylated on tyrosine residues nullifying the inhibitory feedback loop and permitting the downstream activation of AKT (35). In agreement with this, BT474 cells treated with NVP-BE2235 exhibited a decreased mobility shift, stabilization of IRS1, and increased IRS1 tyrosine phosphorylation (Supplementary Fig. S3C). Surprisingly, NVP-BE2235 did not augment IRS1 tyrosine phosphorylation in PTEN knockdown cells. IRS-1 is the major substrate of IGFRI signaling, promoting the activation of downstream effector pathways (36). Recent observations have shown that treatment with the mTOR inhibitor everolimus (RAD001) induces MAPK activation through a negative feedback loop that relies on an S6K-PI3K-Ras-Raf-MEK1/2-dependent mechanism (37). The observed increase in ERK phosphorylation in NVP-BE2235-treated samples is likely to be a consequence of mTOR inhibition, resulting in the suppression of this negative feedback loop.

In contrast, loss of PTEN attenuated AKT dephosphorylation but not S6 dephosphorylation in NVP-BE2235-treated cells. This suggests that at the concentration tested, the inhibitory properties of NVP-BE2235 are insufficient to completely abrogate

the kinase activity of PI3K. In line with these results, treatment of cells with a higher concentration of NVP-BE2235 (500 nmol/L) reduced phosphorylation of AKT⁴⁷³ to levels comparable with those seen in control cell lines (Fig. 5D). These data indicate that only a limited degree of PI3K activity is sufficient to maintain activated AKT in the absence of PTEN phosphatase activity. More importantly, however, the combination treatment of BT474 PTEN knockdown cells with lapatinib and NVP-BE2235 caused a marked decrease in AKT⁴⁷³ phosphorylation similar to that observed with either lapatinib or NVP-BE2235 treatment alone in control cells. Collectively, these data show an additive effect with lapatinib and NVP-BE2235 in cell lines with decreased PTEN expression through the inhibition of both upstream and downstream signaling in the HER2/PI3K/AKT/mTOR axis, accounting for the lethal collaboration exhibited between these two drugs.

NVP-BE2235 suppresses the PI3K-mTOR axis driven by activating mutations in the PI3K pathway in trastuzumab-resistant and lapatinib-resistant cells. Next, we wanted to

examine if NVP-BE2235 would circumvent the observed resistance of breast cancer-relevant mutations toward trastuzumab and lapatinib. Importantly, recent observations have shown that NVP-BE2235 works equally well at repressing the activity of both wt PIK3CA or the two mutant forms, E545K and H1047R (IC₅₀: 4, 4.6, and 5.7 nmol/L, respectively; ref. 38). Retrovirally transduced BT474 cells expressing either wt PIK3CA or the breast cancer-associated PI3K isoforms were treated with either trastuzumab (5 mg/mL), lapatinib (27 nmol/L), NVP-BE2235 (15 nmol/L), or in combination (Fig. 6A). Unsurprisingly, treatment with NVP-BE2235 alone completely inhibited cellular outgrowth of the PI3K mutant-containing cells. These results are in line with previous observations, which show that PI3K mutant cell lines are highly sensitive to mTOR inhibition by rapamycin analogues (29, 39). Similar observations were later confirmed when we quantified the proliferation rates of the PI3K mutant BT474 cell lines (Fig. 6B).

Next, we wanted to determine if treatment with NVP-BE2235 would alleviate the enhanced downstream signaling exhibited in

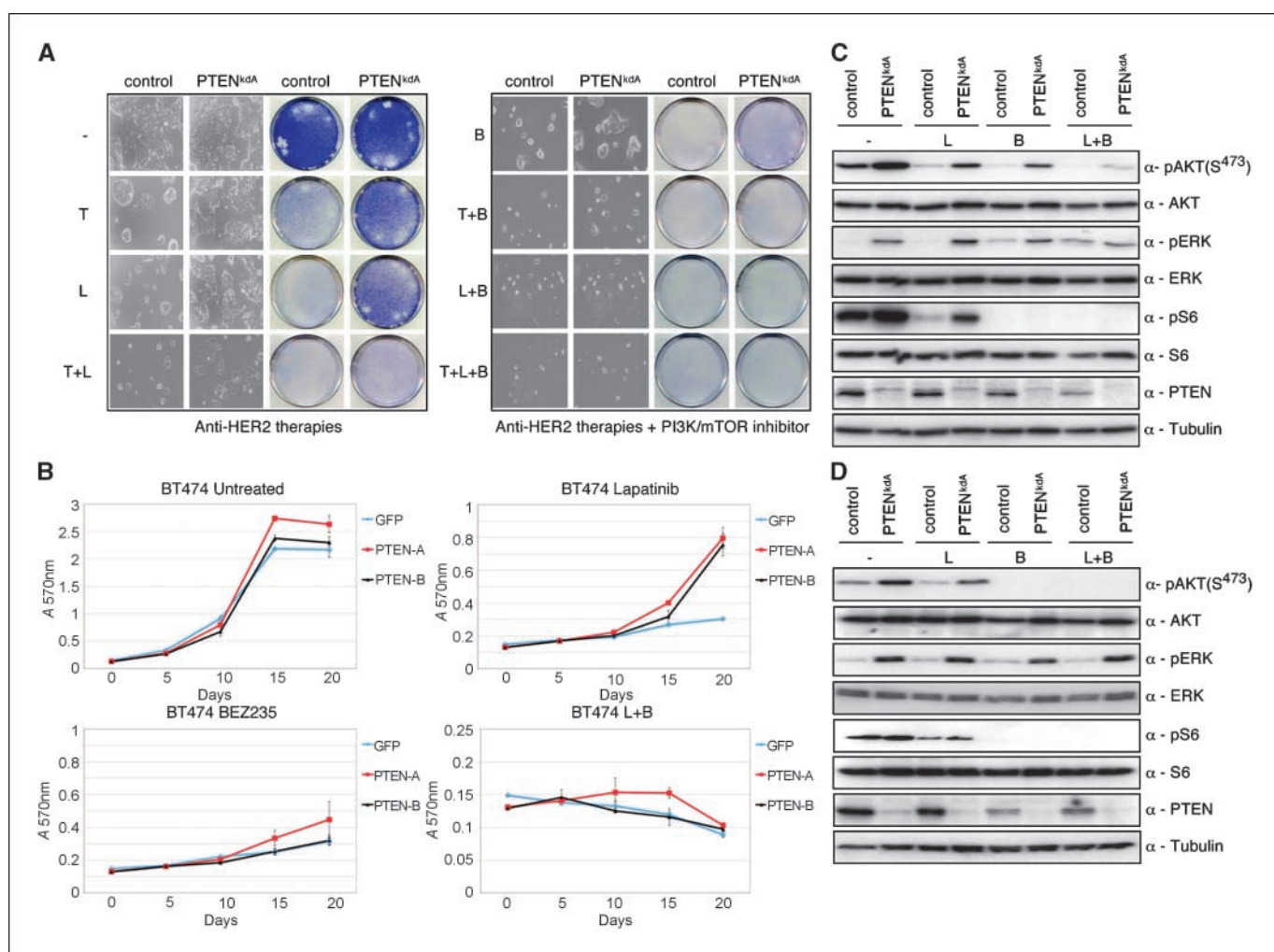


Figure 5. Lapatinib and NVP-BE2235 suppress the PI3K-AKT-mTOR axis driven by loss-of-function PTEN mutations. When required, cells were either treated with trastuzumab (5 μ g/mL), lapatinib (27 nmol/L), or NVP-BE2235 (15 nmol/L), unless otherwise stated. **A**, colony formation assay in BT474 cells infected with either PTEN^{kdA} or relevant controls. Infected cells were treated with trastuzumab, lapatinib, NVP-BE2235, or in combination. After 4 wk, cells were photographed and stained with crystal violet. **B**, growth curves of stably infected PTEN knockdown BT474 cells (PTEN^{kdA} or PTEN^{kdB}) treated for 3 wk with lapatinib, NVP-BE2235, or both. Cell numbers were quantified as described in Materials and Methods. Growth curves were performed in triplicate. Points, mean; bars, SD. **C**, Western blot analysis of stably infected BT474 cells with shRNA PTEN^{kdA} vector treated overnight with lapatinib (27 nmol/L), NVP-BE2235 (100 nmol/L), or both. Whole-cell extracts were analyzed with the indicated antibodies. **D**, Western blot analysis of stably infected BT474 cells with shRNA PTEN^{kdA} vector treated overnight with lapatinib (27 nmol/L), NVP-BE2235 (500 nmol/L), or both. Whole-cell extracts were analyzed with the indicated antibodies.

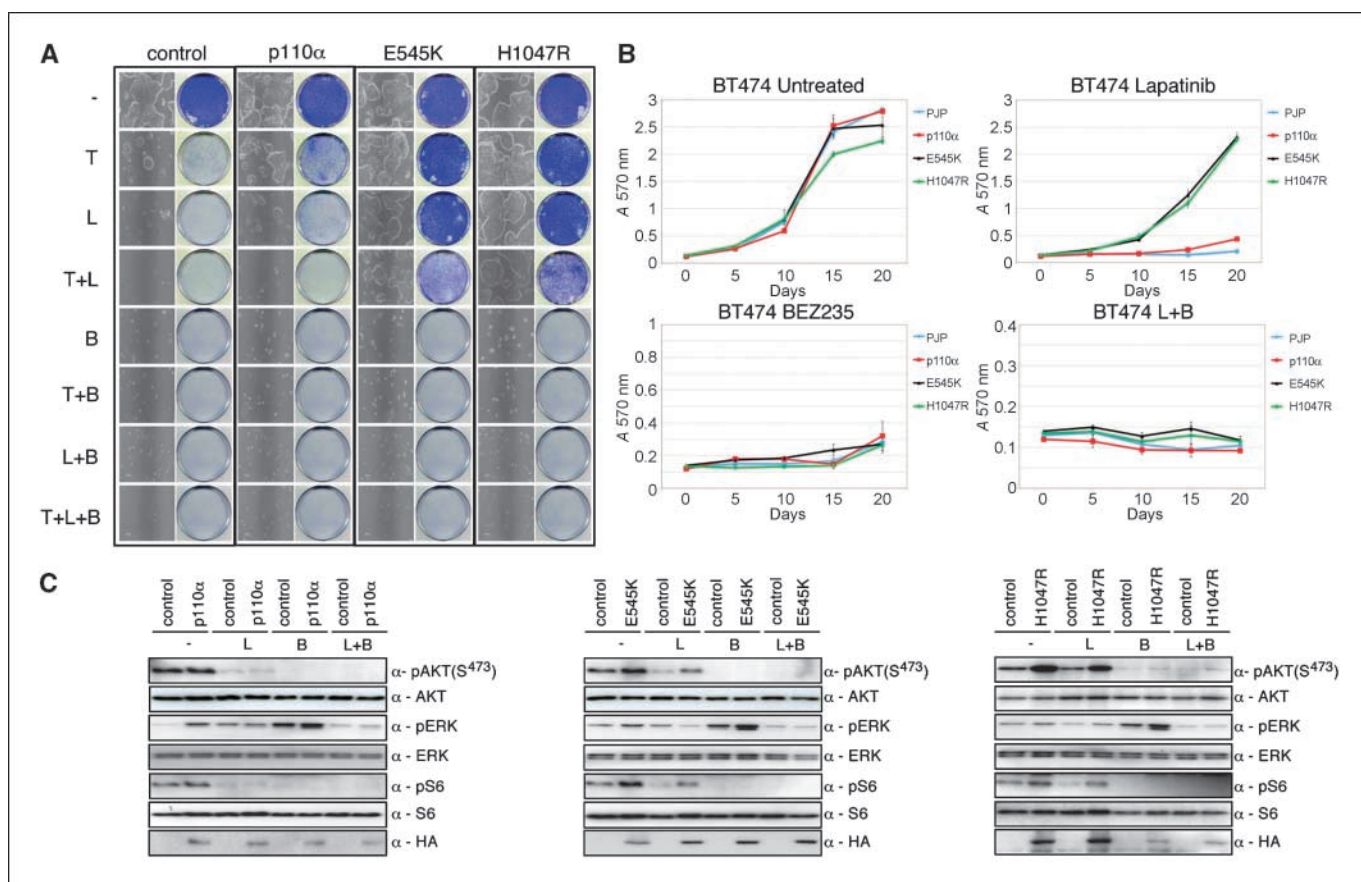


Figure 6. Lapatinib and NVP-BE2235 suppress the PI3K-AKT-mTOR axis driven by gain of function PIK3CA mutations. When required, cells were either treated with trastuzumab (5 μ g/mL), lapatinib (27 nmol/L), or NVP-BE2235 (15 nmol/L), unless otherwise stated. *A*, colony formation assay in BT474 cells infected with either wt PIK3CA α or PIK3CA α mutants E545K and H1047R or relevant controls. Infected cells were treated with trastuzumab, lapatinib, NVP-BE2235, or in combination. After 4 wk, cells were photographed and stained with crystal violet. *B*, growth curves of stably infected PI3K wt or mutant PIK3CA α BT474 cells treated for 3 wk with lapatinib, NVP-BE2235, or both. Cell numbers were quantified as described in Materials and Methods. Growth curves were performed in triplicate. Points, mean; bars, SD. *C*, Western blot analysis of BT474 cells infected with HA-tagged PI3K PIK3CA α (left), PI3K(E545K) PIK3CA α (middle), PI3K(H1047R) PIK3CA α (right), or controls were treated overnight with lapatinib, NVP-BE2235, (100 nmol/L) or both. Whole-cell extracts were analyzed with indicated antibodies.

PI3K mutant cell lines. Indeed NVP-BE2235 treatment alone was sufficient to completely prevent phosphorylation of AKT⁴⁷³ and S6^{240/244} to levels comparable with those seen in control cell lines (Fig. 6C). Furthermore, these data show that treatment with NVP-BE2235 overcomes PI3K-dependent lapatinib resistance in BT474 cells.

Discussion

Lapatinib is approved for the therapy of patients with HER2-positive breast cancer who have progressed on trastuzumab. However, the effectiveness of this compound is limited by both primary and acquired resistance. To identify novel mechanisms of resistance to lapatinib, we have performed a genome-wide loss-of-function shRNA screen. Here, we have identified the tumor suppressor PTEN as a mediator of lapatinib sensitivity *in vitro* and *in vivo*. Previous reports have shown that lapatinib activity is not dependent upon PTEN (19, 40). However, using an unbiased approach, we clearly show that loss of PTEN and the resulting activation of the PI3K pathway lead to deregulation of lapatinib sensitivity in our model. Consistent with this, we have identified that the two most prevalent breast cancer mutations in PIK3CA (E545K and H1047R) also confer resistance to lapatinib. Therefore, hyperactivation of the PI3K pathway by either loss of PTEN

function or activating mutations of PI3K result in resistance to lapatinib. In addition, our findings are consistent with recently reported observations using the anti-HER2 monoclonal antibody trastuzumab (4, 13). However, it must be noted that, whereas overexpression of wt PIK3CA diminished the effectiveness of trastuzumab in BT474 cells, it was unable to circumvent the growth inhibitory properties of lapatinib, suggesting that lapatinib may function as a single agent in patients overexpressing wt PIK3CA.

A number of possibilities might explain the differing effect of PTEN loss and lapatinib resistance observed between our group and others, including the efficiency of PTEN knockdown in targeted cell lines, the use of stably infected cell lines to determine the long-term effects of PTEN knockdown and lapatinib treatment, and the use of a 20-fold lower dose of lapatinib in the initial screen, reducing the chance of nonspecific effects. Be that as it may, a number of studies have identified that PTEN loss does not predict for lapatinib response in patients (19, 40). Similar results have been observed in trastuzumab resistance, whereby no significant correlation has been observed in PTEN loss and time to progression in trastuzumab-treated patients (13). These data indicate that a larger cohort of patients may be needed to observe differences in response in PTEN-deficient tumors. An additional explanation is the lack of a validated test to determine PTEN

loss in human tumors. Until a validated test becomes available, it will be difficult to try to establish reliable clinical correlations between PTEN loss and response to lapatinib and other agents. However, subsequent analysis combining both PTEN status and PI3K status has clearly shown the potential of PI3K pathway hyperactivation as a biomarker for trastuzumab efficacy. As such, it will be of critical importance to equally assess PI3K pathway hyperactivation as a predictor to lapatinib response.

Abnormal activation of the PI3K pathway is frequent in breast cancer. Loss-of-function PTEN or PIK3CA mutations have been observed in ~20% to 25% and 18% to 40% of primary breast cancers, respectively (13, 14, 29). Taking into consideration the nearly mutual exclusivity between loss-of-function PTEN mutations and PI3K mutations (14), it is not surprising that deregulation of the PI3K pathway likely occurs in over 50% of breast cancers (29). In addition, a significant correlation between HER2 overexpression and the presence of PI3K mutations has been described (14).

There are several potential implications of these observations. One such implication is that PTEN status and the presence of PI3K activating mutations should be taken into account in clinical studies with anti-HER2 agents because they could predict for resistance. A second consequence of our findings is that hyperactivation of the PI3K pathway may be pharmacologically targeted, which could in turn result in reversal of lapatinib resistance. This has been a focus of our study. We have shown a nearly complete loss of PI3K downstream signaling in BT474 cells, harboring a deregulated PI3K pathway upon treatment with the dual PI3K/mTOR inhibitor NVP-BE235 and lapatinib. Interestingly, treatment of NVP-BE235 alone in PI3K mutant cell lines was sufficient to inhibit AKT phosphorylation. This is in contrast to cells with PTEN loss, wherein the same NVP-BE235 dose fails to completely abrogate AKT activity. Considering PI3K mutant cell lines retain PTEN, this result highlights a collaboration between mechanisms to down-regulate signaling through the cascade—NVP-BE235 inhibiting PIK3CA and PTEN dephosphorylating its downstream target PIP3. Ultimately, this could affect clinical decision-making, wherein lower doses of NVP-BE235 may be selected for patients harboring activating mutations of PI3K, with higher doses for those individuals with PTEN loss.

Recent data have highlighted the use of the PI3K inhibitors LY294002 and wortmannin in the restoration of trastuzumab sensitivity in PTEN-deficient cells (4). However, the use of these compounds in the clinic has been limited by their poor pharmacokinetics and excessive toxicity (reviewed in ref. 41). Similarly, the use of rapamycin in patients with an activated PI3K pathway has shown promising results in clinical trials (42). Again, however, patients who rapidly progressed on rapamycin treatment exhibited enhanced PRAS40 phosphorylation, a downstream target of AKT. Although highly promising, these data suggest that rapamycin efficacy in patients is limited due to the inhibition of the negative feedback loop.

Here, our data suggest that combination therapy with NVP-BE235, which is in early-stage clinical trials, and lapatinib should be considered in patients whose tumors have a defined deregulated PI3K pathway.

Deciphering the molecular basis of response to lapatinib and other HER2-directed therapies is of great importance to maximizing the clinical efficacy of these compounds. In this present study, we show the power of genome-wide loss of function screens to identify critical components of lapatinib sensitivity. Furthermore, our data justify the need for future clinical trials to validate the PI3K pathway as a biomarker for lapatinib sensitivity and explore a combined blockade with anti-PI3K inhibitors and lapatinib in a selected patient population with tumors with HER2 amplification and hyperactivation of the PI3K pathway by PTEN deletion or activating PI3K mutations.

Disclosure of Potential Conflicts of Interest

J. Baselga: speakers bureau/honoraria, Novartis.

Acknowledgments

Received 5/9/2008; revised 8/4/2008; accepted 9/4/2008.

Grant support: Breast Cancer Research Foundation and NIH. Dr. Baselga is currently involved in conducting clinical trials sponsored by Hoffman-La Roche, GlaxoSmithKline, and Novartis. The sponsors are not responsible for the study design, data collection and analysis, interpretation of data, or preparation of the manuscript.

The costs of publication of this article were defrayed in part by the payment of page charges. This article must therefore be hereby marked *advertisement* in accordance with 18 U.S.C. Section 1734 solely to indicate this fact.

We thank Ben Markman for the critical reading of this manuscript.

References

- Slamon DJ. Studies of the HER-2/neu proto-oncogene in human breast cancer. *Cancer Invest* 1990;8:253.
- Slamon DJ, Clark GM, Wong SG, Levin WJ, Ullrich A, McGuire WL. Human breast cancer: correlation of relapse and survival with amplification of the HER-2/neu oncogene. *Science* 1987;235:177–82.
- Marmor MD, Yarden Y. Role of protein ubiquitylation in regulating endocytosis of receptor tyrosine kinases. *Oncogene* 2004;23:2057–70.
- Nagata Y, Lan KH, Zhou X, et al. PTEN activation contributes to tumor inhibition by trastuzumab, and loss of PTEN predicts trastuzumab resistance in patients. *Cancer Cell* 2004;6:117–27.
- Shin I, Yakes FM, Rojo F, et al. PKB/Akt mediates cell-cycle progression by phosphorylation of p27(Kip1) at threonine 157 and modulation of its cellular localization. *Nat Med* 2002;8:1145–52.
- Clynes RA, Towers TL, Presta LG, Ravetch JV. Inhibitory Fc receptors modulate *in vivo* cytotoxicity against tumor targets. *Nat Med* 2000;6:443–6.
- Baselga J, Tripathy D, Mendelsohn J, et al. Phase II study of weekly intravenous recombinant humanized anti-p185HER2 monoclonal antibody in patients with HER2/neu-overexpressing metastatic breast cancer. *J Clin Oncol* 1996;14:737–44.
- Cobleigh MA, Vogel CL, Tripathy D, et al. Multinational study of the efficacy and safety of humanized anti-HER2 monoclonal antibody in women who have HER2-overexpressing metastatic breast cancer that has progressed after chemotherapy for metastatic disease. *J Clin Oncol* 1999;17:2639–48.
- Lu Y, Zi X, Zhao Y, Mascarenhas D, Pollak M. Insulin-like growth factor-I receptor signaling and resistance to trastuzumab (Herceptin). *J Natl Cancer Inst* 2001;93:1852–7.
- Sergina NV, Rausch M, Wang D, et al. Escape from HER-family tyrosine kinase inhibitor therapy by the kinase-inactive HER3. *Nature* 2007;445:437–41.
- Scaltriti M, Rojo F, Ocana A, et al. Expression of p95HER2, a truncated form of the HER2 receptor, and response to anti-HER2 therapies in breast cancer. *J Natl Cancer Inst* 2007;99:628–38.
- Samuels Y, Wang Z, Bardelli A, et al. High frequency of mutations of the PIK3CA gene in human cancers. *Science* 2004;304:554.
- Berns K, Horlings HM, Hennessy BT, et al. A functional genetic approach identifies the PI3K pathway as a major determinant of trastuzumab resistance in breast cancer. *Cancer Cell* 2007;12:395–402.
- Saal LH, Holm K, Maurer M, et al. PIK3CA mutations correlate with hormone receptors, node metastasis, and ERBB2, and are mutually exclusive with PTEN loss in human breast carcinoma. *Cancer Res* 2005;65:2554–9.
- Rusnak DW, Lackey K, Affleck K, et al. The effects of the novel, reversible epidermal growth factor receptor/ErbB-2 tyrosine kinase inhibitor, GW2016, on the growth of human normal and tumor-derived cell lines *in vitro* and *in vivo*. *Mol Cancer Ther* 2001;1:85–94.
- Nahta R, Yuan LX, Du Y, Esteva FJ. Lapatinib induces apoptosis in trastuzumab-resistant breast cancer cells: effects on insulin-like growth factor I signaling. *Mol Cancer Ther* 2007;6:667–74.
- Konecny GE, Pegram MD, Venkatesan N, et al. Activity of the dual kinase inhibitor lapatinib (GW572016) against HER-2-overexpressing and trastuzumab-treated breast cancer cells. *Cancer Res* 2006;66:1630–9.
- Geyer CE, Forster J, Lindquist D, et al. Lapatinib plus capecitabine for HER2-positive advanced breast cancer. *N Engl J Med* 2006;355:2733–43.
- Johnston S, Trudeau M, Kaufman B, et al. Phase II study of predictive biomarker profiles for response

- targeting human epidermal growth factor receptor 2 (HER-2) in advanced inflammatory breast cancer with lapatinib monotherapy. *J Clin Oncol* 2008;26:1066–72.
20. van der Eb AJ, Graham FL. Assay of transforming activity of tumor virus DNA. *Methods Enzymol* 1980;65: 826–39.
 21. Baselga J, Norton L, Albanell J, Kim YM, Mendelsohn J. Recombinant humanized anti-HER2 antibody (Herceptin) enhances the antitumor activity of paclitaxel and doxorubicin against HER2/neu overexpressing human breast cancer xenografts. *Cancer Res* 1998;58: 2825–31.
 22. Berns K, Hijmans EM, Mullenders J, et al. A large-scale RNAi screen in human cells identifies new components of the p53 pathway. *Nature* 2004;428:431–7.
 23. Rusnak DW, Alligood KJ, Mullin RJ, et al. Assessment of epidermal growth factor receptor (EGFR, ErbB1) and HER2 (ErbB2) protein expression levels and response to lapatinib (Tykerb, GW572016) in an expanded panel of human normal and tumor cell lines. *Cell Prolif* 2007;40: 580–94.
 24. Brummelkamp TR, Fabius AW, Mullenders J, et al. An shRNA barcode screen provides insight into cancer cell vulnerability to MDM2 inhibitors. *Nat Chem Biol* 2006;2: 202–6.
 25. Kortlever RM, Higgins PJ, Bernards R. Plasminogen activator inhibitor-1 is a critical downstream target of p53 in the induction of replicative senescence. *Nat Cell Biol* 2006;8:877–84.
 26. Xia W, Gerard CM, Liu L, Baudson NM, Ory TL, Spector NL. Combining lapatinib (GW572016), a small molecule inhibitor of ErbB1 and ErbB2 tyrosine kinases, with therapeutic anti-ErbB2 antibodies enhances apoptosis of ErbB2-overexpressing breast cancer cells. *Oncogene* 2005;24:6213–21.
 27. Burris HA III, Hurwitz HI, Dees EC, et al. Phase I safety, pharmacokinetics, and clinical activity study of lapatinib (GW572016), a reversible dual inhibitor of epidermal growth factor receptor tyrosine kinases, in heavily pretreated patients with metastatic carcinomas. *J Clin Oncol* 2005;23:5305–13.
 28. Cantley LC, Neel BG. New insights into tumor suppression: PTEN suppresses tumor formation by restraining the phosphoinositide 3-kinase/AKT pathway. *Proc Natl Acad Sci U S A* 1999;96:4240–5.
 29. Isakoff SJ, Engelman JA, Irie HY, et al. Breast cancer-associated PIK3CA mutations are oncogenic in mammary epithelial cells. *Cancer Res* 2005;65: 10992–1000.
 30. Miled N, Yan Y, Hon WC, et al. Mechanism of two classes of cancer mutations in the phosphoinositide 3-kinase catalytic subunit. *Science* 2007;317:239–42.
 31. Zhao JJ, Liu Z, Wang L, Shin E, Loda MF, Roberts TM. The oncogenic properties of mutant p110 α and p110 β phosphatidylinositol 3-kinases in human mammary epithelial cells. *Proc Natl Acad Sci U S A* 2005;102: 18443–8.
 32. Maira SM, Stauffer F, Brueggen J, et al. Identification and characterization of NVP-BEZ235, a new orally available dual phosphatidylinositol 3-kinase/mammalian target of rapamycin inhibitor with potent *in vivo* antitumor activity. *Mol Cancer Ther* 2008;7:1851–63.
 33. Serra V, Markman B, Scaltriti M, et al. NVP-BEZ-235, a dual PI3K/mTOR inhibitor, prevents PI3K signaling and inhibits growth of cancer cells with activating PI3K mutations. *Proceedings of the 99th Annual Meeting of the American Association for Cancer Research* 2008.
 34. Pederson TM, Kramer DL, Rondinone CM. Serine/Threonine Phosphorylation of IRS-1 Triggers Its Degradation. *Diabetes* 2001;50:24–31.
 35. O'Reilly KE, Rojo F, She QB, et al. mTOR inhibition induces upstream receptor tyrosine kinase signaling and activates Akt. *Cancer Res* 2006;66:1500–8.
 36. Bjornsti MA, Houghton PJ. The TOR pathway: a target for cancer therapy. *Nat Rev Cancer* 2004;4:335–48.
 37. Carracedo A, Ma L, Teruya-Feldstein J, et al. Inhibition of mTORC1 leads to MAPK pathway activation through a PI3K-dependent feedback loop in human cancer. *J Clin Invest* 2008;118:3065–74.
 38. Maira S, Stauffer F, Brueggen J, et al. Identification and characterization of NVP-BEZ235 a new orally available dual phosphatidylinositol 3-kinase/mammalian target of rapamycin inhibitor with potent *in vivo* antitumor activity. *Mol Cancer Ther* 2008;7:1851–63.
 39. Bader AG, Kang S, Vogt PK. Cancer-specific mutations in PIK3CA are oncogenic *in vivo*. *Proc Natl Acad Sci U S A* 2006;103:1475–9.
 40. Xia W, Husain I, Liu L, et al. Lapatinib antitumor activity is not dependent upon phosphatase and tensin homologue deleted on chromosome 10 in ErbB2-overexpressing breast cancers. *Cancer Res* 2007;67:1170–5.
 41. Marone R, Cmiljanovic V, Giese B, Wymann MP. Targeting phosphoinositide 3-kinase-moving towards therapy. *Biochim Biophys Acta* 2008;1784:159–85.
 42. Cloughesy TF, Yoshimoto K, Nghiemphu P, et al. Antitumor activity of rapamycin in a Phase I trial for patients with recurrent PTEN-deficient glioblastoma. *PLoS Med* 2008;5:e8.